BIOMASS AND BIOENERGY 69 (2014) 276–286

Available online at www.sciencedirect.com

ScienceDirect

http://www.elsevier.com/locate/biombioe

Steam gasification of rapeseed, wood, sewage sludge and miscanthus biochars for the production of a hydrogen-rich syngas

Anwar Sattar [a], *Gary A. Leeke* [a], *Andreas Hornung* [b], *Joseph Wood* [a,*]

[a] *School of Chemical Engineering, University of Birmingham, Edgbaston, Birmingham B15 2TT, UK*
[b] *Fraunhofer Institute, UMSICHT, An der Maxhutte 1, 92237 Sulzbach Rosenberg, Germany*

ARTICLE INFO

Article history:
Received 4 April 2014
Received in revised form
16 July 2014
Accepted 22 July 2014
Available online 20 August 2014

Keywords:
Biochar steam gasification
Intermediate pyrolysis
Brassica napus
Sewage sludge
Miscanthus x giganteus
Pinus sylvestris – Picea sitchensis

ABSTRACT

Steam gasification of biochars has emerged as a promising method for generating syngas that is rich in hydrogen. In this study four biochars formed via intermediate pyrolysis (wood pellet, sewage sludge, rapeseed and miscanthus) were gasified in a quartz tubular reactor using steam. The dynamic behaviour of the process and effects of temperature, steam flow and particle size were studied. The results show that increases in both steam flow and temperature significantly increase the dry gas yield and carbon conversion, but hydrogen volume fraction decreases at higher temperatures whilst particle size has little effect on gaseous composition. The highest volume fraction of hydrogen, 58.7%, was obtained at 750 °C from the rapeseed biochar.

© 2014 The Authors. Published by Elsevier Ltd. This is an open access article under the CC BY license (http://creativecommons.org/licenses/by/3.0/).

1. Introduction

As the move towards sustainable energy generation gathers pace, renewable technologies are being implemented all over the world and the UK is no exception. According to the Department of Energy and Climate Change (DECC), renewable electricity accounted for 9.4% of the total electricity generated during 2011 and renewable energy as a whole accounted for 3.8% of the UK's total energy supply; an increase from 3.2% in 2010 [1]. Biomass use in particular is increasing rapidly as a result of its versatility in feedstock and applications, which covers a wide range from direct combustion for heat and power, biofuel synthesis to value added chemicals. In 2010, bioenergy accounted for 38% of the total renewable energy generated in the UK. This share is set to increase as coal power stations such as Tilbury B are converted from coal to dedicated biomass burners [1]. In order to maximise the use of available feedstock, advanced thermochemical technologies such as pyrolysis and gasification must be utilised, since these technologies enable low quality biomass fuels and residues to be upgraded into more valuable forms [2].

* *Corresponding author*. Tel.: +44 0 121 414 5295; fax: +44 0 121 414 5234.
E-mail addresses: AXS164@bham.ac.uk (A. Sattar), g.a.leeke@bham.ac.uk (G.A. Leeke), andreas.hornung@umsicht.fraunhofer.de (A. Hornung), j.wood@bham.ac.uk, joe_wood99@hotmail.com (J. Wood).
http://dx.doi.org/10.1016/j.biombioe.2014.07.025
0961-9534/© 2014 The Authors. Published by Elsevier Ltd. This is an open access article under the CC BY license (http://creativecommons.org/licenses/by/3.0/).

Pyrolysis is described as the thermal decomposition of carbonaceous matter into a range of useful products, in the absence of an oxidising agent. It is carried out at medium to high temperatures (350–650 °C) and gives three products; liquids (bio-oil), gases (CO, CO_2, H_2, CH_4 up to C_6H_6) and char (biochar if biomass is the starting material) [3]. Three modes of pyrolysis have been developed – slow, fast and a new type, intermediate pyrolysis. Heating rates used in the process define the mode of pyrolysis. Table 1 compares the three modes [2] [4].

Slow pyrolysis or carbonisation is used to produce biochar whilst fast pyrolysis is optimised to produce bio-oil. These processes are commercially important as the products can be used in a variety of processes such as combined heat and power (CHP) generation, biofuels and chemicals [2]. Although successful applications have been developed with woody biomass, non-woody biomass can lead to bituminous products which solidify at room temperature [5]. Intermediate pyrolysis enables a diverse range of products such as waste wood, food waste, grass and algae to be utilised [5]. One type of intermediate pyrolysis utilises the pyroformer reactor. It comprises counter rotating coaxial screws to move the feed along the reactor and allows for easy control of solid residence time. Heat transfer is aided by the use of metal spheres, negating the need for costly feed preparation associated with fast pyrolysis [6].

The biochars produced from intermediate pyrolysis have a high carbon content, low volatile content and are reactive enough to be gasified by either steam or CO_2 [7]. Many reactions occur during the steam gasification process. The main ones are shown in Table 2 below.

Interest in the area of steam gasification of biochars has grown considerably. Yan et al. [9] carried out steam gasification experiments of pine sawdust biochar in a fixed bed reactor. They reported an increase in hydrogen volume fraction with increasing temperature as a result of further cracking, and at 850 °C, 52.4% hydrogen (on a dry basis) was obtained, with a steam flow of 165 g min^{-1} kg^{-1} biochar. In another study [10], the same authors investigated the effects of particle size and temperature on biochar derived from the fast pyrolysis of cyanobacterial blooms. They reported that varying the particle size had little effect on the gaseous composition or the yield of gas produced. Chaudhari et al. [7] gasified bagasse biochar using steam and reported a maximum hydrogen volume fraction of 51.2%. In another study [11], the same authors gasified bagasse and commercial biochars in a fixed bed microreactor. They reported a very high hydrogen volume fraction (76.2%) at 700 °C and low steam flow rates (20.8 g min^{-1} kg^{-1} char), which decreased to 70% at 800 °C at the same steam flow rate. At higher steam flow rates (167 g min^{-1} kg^{-1} char), no overall trend was reported in the hydrogen content as it behaved differently with respect to the chars tested. Zhang et al. [12] scaled up biochar gasification using a fluidised bed reactor and reported that although the volume fraction of hydrogen increases slightly with increasing temperature from 750 to 900 °C, no clear trend was reported.

The above investigations were all carried out using biochars from fast pyrolysis. Significant differences exist between pyrolysis modes and these differences have a major effect on the biochars produced. For example, Chen et al. [13] investigated the reactivity of biomass chars from rapid and slow pyrolysis using steam and CO_2. They reported that chars from rapid pyrolysis showed a reactivity that was three times higher than those formed by slow pyrolysis. Previous studies have also failed to provide a link between the physico–chemical properties of the biochars and their behaviours during the steam gasification process. The main aim of this study was to investigate whether four biochars; wood pellet biochar (WPB), rapeseed biochar (RSB), sewage sludge biochar (SSB) and miscanthus biochar (MCB), all formed via intermediate pyrolysis, can be used to produce a high quality syngas that is rich in hydrogen. Other aims include finding the optimum conditions to produce such a gas; determining which biochar is most suitable for hydrogen production and; to determine the physico-chemical effects of the biochar on the gasification process and to shed new light on the dynamic gasification behaviour.

2. Materials and methods

The biochars used in the study were produced in the Pyroformer at Aston University, using intermediate pyrolysis and the gasification studies were carried out at the University of Birmingham. The precursor biomass substrates were acquired

Table 1 – Comparison of the three modes of pyrolysis [2,4].

Pyrolysis mode	Conditions	Product distribution (g kg^{-1} initial dry feedstock)		
		Liquid	Char	Gas
Fast	Reactor temperature: ~500 °C Heating Rates: >1000 °C s^{-1} Hot vapour residence time: ~1 s Solid residence time: ~1 s	750	120	130
Intermediate	Reactor temperature ~ 400–500 °C Heating rate range: 1–1000 °C s^{-1} Hot vapour residence time ~ 10–30 s Solid residence time: 1–30 min	500	250	250
Slow	Reactor temperature ~ 300–500 °C Heating rate: up to 1 °C s^{-1} Solid residence times: ~ hours–days.	300	350	350

Table 2 – Reaction and Enthalpy of Reaction at 298 K and 101.3 kPa [8,9].

Reaction	Enthalpy of reaction (kJ mol^{-1})	Reaction equation No
$C_x H_y O_z \rightarrow aCO_2 + bH_2O + cCH_4 + dCO + eH_2 + fC_2$ (pyrolysis)		1
$CO_2 + C \rightleftharpoons 2CO$	+172	2
$C + H_2O \rightleftharpoons CO + H_2$	+131	3
$C + ½O_2 \rightarrow CO$	−111	4
$CH_4 + H_2O \rightleftharpoons CO + 3H_2$	+206	5
$CO + H_2O \rightleftharpoons CO_2 + H_2$	−41.2	6
$C + 2H_2 \rightleftharpoons CH_4$	−74.8	7

and cultivated from the following companies and/or locations; anaerobically digested sewage sludge, Severn Trent Water Ltd (Midlands, UK); rapeseed (seeds), Allgäu, Germany; Miscanthus (stalk) harvested in Shropshire, UK, Agripellets Ltd; wood pellets (debarked mixture of pine and spruce), Midlands Bio Energy Ltd (wood sourced from Forest Stewardship Council, Scotland).[1] The substrates were received in sealable bags in which they were kept in desiccators in a moisture free, low light, air environment. All the biochars were produced at a pyroformer temperature of 500 °C except the WPB which was produced at 450 °C. The particle size distribution of the biochars on a mass basis (g g^{-1}) was as follows; WPB, 47.6% pellets and 52.4% broken pellets/shavings. Average pellet length is 7.88 mm and 'oily' nature of the biochar causes coalescence of some particles. RSB appears as miniature versions of rapeseed seeds alongside broken and powder particles; 42% with diameter >850 μm, 40% in the range 300–850 μm and 18% < 300 μm. SSB consists of dense cylindrical pellets with 4.9 mm average diameter of which 85.3% are between 5 and 15 mm long. MCB is a mixture of cylindrical pellets alongside broken pellets with some in powder form. The pellets have varying mean diameters, larger pellets having a mean diameter of 9.6 mm and smaller pellets 6.74 mm. On average, 68.15% of the pellets had a mean diameter >8.5 mm, 12.23% in the range 0.85–8.5 mm and the rest <0.85 mm (850 μm).

2.1. Biochar characterisation

Elemental analysis was carried out by MEDAC Ltd, Surrey, UK. Mineral content was determined by X-Ray Fluorescence (XRF) Spectroscopy using the pellet press method. 500 mg biochar was crushed and mixed with 100 mg of inert wax and pressed into a pellet. A Bruker S8 Tiger XRF Analyser was used to carry out the analysis. Volatile content was determined according ASTM D1762-84 [14]. Biochar was crushed and sieved through a 250 μm sieve. One gram ±0.1 mg was weighed in a preheated crucible (with lid) and placed onto the ledge of a Carbolite CWF 1300 muffle furnace that was heated to 950 °C. The furnace door was opened, after 2 min, the crucible was moved onto the edge of the furnace and after a further 3 min, the crucible was placed at the rear of the furnace with the door shut and kept there for 6 min. It was then cooled and weighed. Scanning electron microscopy (SEM) was used to analyse the surface topography and structure of the biochars. A representative sample was mounted onto a metallic disc without any processing, and analysed using a Phillips XL30ESEM.

2.2. Biochar gasification

Biochars were gasified in a quartz tubular reactor; $L = 750$ mm, $D = 60$ and a 19 mm section (see insert of Fig. 1) with a B19 socket joint. The quartz sample holder; $L = 550$ mm, $D = 16$ mm and had a section of 320 mm length hollowed out to allow the char to be placed upon it and a corresponding B19 cone which forms a gas tight seal with the reactor. Upstream of the reactor was a pump and a heated line to produce steam, a preheater to superheat the steam, a N_2 line to purge the reactor and a thermocouple placed inside the reactor. Downstream, there were two condensers, one was connected to a tar collector where most of the condensate is collected, the second ensures no vapours remain in the gas stream and the filters clean the gas of any particulates. A bubble flow meter was used for gas flowrate measurements and the gas was collected in a gas bag or vented to atmosphere via extraction. The set up is shown in Fig. 1.

Each experiment was carried out as follows; 3 g of biochar was weighed and placed onto the sample holder. The preheater, furnace and condenser were switched on. After achieving desired temperatures, the steam generation kit was switched on. When steam began to flow out of the reactor, the system was purged with N_2 at a flow rate of 600 ml min^{-1}. After 15 min, the sample holder was inserted into the reactor and N_2 was switched off. Gas collection was performed using two methods; by a gas bag or 30 ml serum bottles were used as reservoirs to obtain a representative sample at gasification times of 1, 3, 5, 7.5, 10, 15, 20, 25 and 30 min. A correction factor was calculated to account for the dissolution of CO_2 in the water using standard gas mixtures. After 30 min, the reaction was stopped and the furnace, preheater, heated line and pump were switched off. The reactor was purged with N_2 for a further 10 min. The spent biochars (those produced at 650, 750, 850 °C and 54 and 277 g min^{-1} kg^{-1} biochar) were sent to MEDAC Labs Ltd for further elemental analyses.

The biochars were gasified in their original form unless stated; experiments were performed in order to study (i) the effects of differing particle sizes, (ii) the selection of the biochar most suitable for gasification and (iii) their effects on efficiency. Each experiment was carried out three times and the average results are shown.

[1] This work was performed on commercially available biomass substrates. As a result, the full chain of custody cannot be ascertained. However, the authors believe that the work exemplifies the difference between typically available materials and waste suitable for gasification, although substrate factors may affect results.

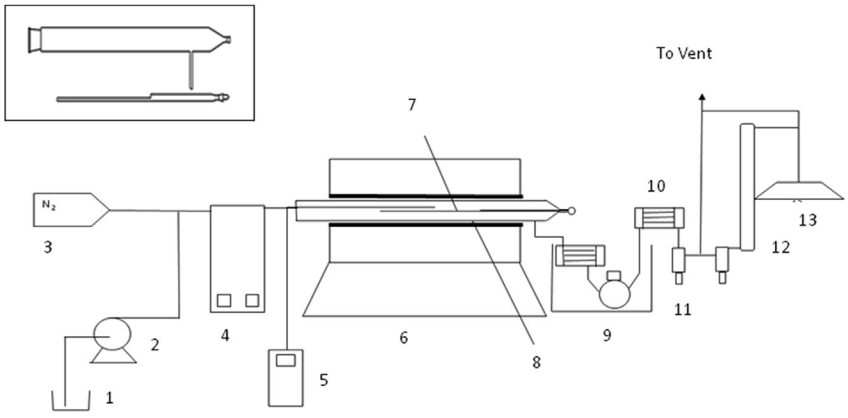


Fig. 1 – Experimental set up; 1. Water Reservoir; 2. Pump and heated line; 3. N_2 line; 4. Preheater; 5. Temperature read out; 6. Electric furnace; 7. Quartz sample holder; 8. Quartz reactor; 9. Primary condenser and tar trap; 10. Secondary condenser; 11. Water traps and filters; 12. Bubble flow meter; 13. Gas collection kit. [insert; reactor and sample holder].

2.3. *Gas analysis*

Gases were analysed using an Agilent 7890A Refinery Gas Analyser. The 7890A has three detectors, one flame ionising detector (FID) for hydrocarbons and two thermal conductivity detectors (TCD) – one for hydrogen and one for permanent gases.

2.4. *Methods of data processing*

Carbon conversion (CC) and carbon conversion efficiency (CCE) are defined as; moles of carbon lost from the biochar during the reaction; and, moles of carbon converted into syngas, respectively. They are calculated as follows;

$$CC(\%) = [1 - (C_o/C_i)] \times 100 \quad (8)$$

$$CCE(\%) = \left[\left(\sum n_i \cdot V\right)/C_i\right] \times 100 \quad (9)$$

where; C_o and C_i are moles of carbon 'out' and 'in' respectively, n_i is the moles of carbon in component i and V is the total volume of gas produced.

Higher heating value (HHV), dry gas yield (DGY) and reactivity (R) are calculated as follows;

$$HHV(MJ\ m^{-3}) = \left(\sum X_i\ H_i\right) \quad (10)$$

$$DGY(m^3 kg^{-1}) = V/3000 \quad (11)$$

$$R(\%\ min^{-1}) = 1/m\ dm/dt \quad (12)$$

where X is the volume fraction of component i in the gas mixture and H is the corresponding higher heating value. R is reactivity and m is mass.

3. Results and discussion

3.1. *Elemental and mineral content*

Table 3 shows the ultimate analysis and mineral contents of the biochars. The low carbon content of the SSB is as a result of it being processed in an anaerobic digester before being pyrolysed. The MCB and RSB have similar amounts of carbon

Table 3 – Analysis of the biochars.

	Biochar ultimate analysis (g kg^{-1})				Mineral	Biochar mineral content (g kg^{-1})			
	Wood pellet	Rapeseed	Sewage sludge	Miscanthus		Wood pellet	Rapeseed	Sewage sludge	Miscanthus
C	716	603	30	622	Ca	10.7	81.9	125	62.4
H	46.2	40	41.9	43.7	K	7.7	92.8	11.3	42.4
N	5.4	42	18.3	8	Fe	30.8	8.7	75.6	33.4
S	2.2	1	8.8	2.8	Si			80.7	31.8
Ash	26.4	42	355	103	P		53.6	50.2	4.1
O[a]	203.8	272	276	220.5	Al			44	
Volatile content (g kg^{-1})	612	215	216	309					
HHV[b] (MJ kg^{-1})	28.8	24	11	24.7					

[a] By difference.
[b] Higher heating value (Equation (10)).

and hydrogen but differing amounts of nitrogen and ash. The high carbon and volatile content of the WPB is as a result of its lower temperature of production. Both SSB and RSB had similar volatile contents at just over 21%. Mineral content, in particular alkali and alkaline earth metallic (AAEM) species, have been shown to enhance biochar reactivity [15]. Their activity is reported to be K > Na > Ca [16]. In this respect, the RSB contains the most AAEM per unit mass whilst WPB contains the least. Sewage sludge reactivity is enhanced by the presence of species such as Fe, which can catalyse gasification reactions and increase hydrogen yield [17].

3.2. *Scanning electron microscopy*

Surface topography of the four biochars is shown in the SEM micrographs in Fig. 2. Each biochar has a unique surface which could affect its behaviour during gasification. Both the RSB and MCB have porous structures which are in stark contrast to the WPB and SSB which are solid and non-porous and could offer resistance to steam diffusivity. Porosity of the biochar is affected by the rate at which the devolatilisation occurs during pyrolysis [18] which in turn is affected by the AAEM content and temperature of pyrolysis [16]. The high AAEM content may explain why the RSB and MCB have such porous structures compared to WPB and SSB.

3.3. *Dynamic aspects of the gasification process*

Previous studies have split steam gasification into two stages; (i) devolatilisation and (ii) gasification. Devolatilisation is thought to occur first, leading to tar, char and volatiles, followed by gasification where reactions 2–6 compete with one another [9]. Fig. 3 a and b illustrates that at 850 °C, both stages occur simultaneously. At higher steam flows, an increase in the initial product flowrate (at 1 min) is observed; suggesting that both pyrolysis and gasification reactions are occurring together. In all cases, increases in temperature leads to significant increases in product flowrates as gasification reactions become less kinetically limited as a result of increases in rate constants. Due to its high volatile content, the WPB produces the highest mass of gas in the first minute; its flowrate then falls sharply and remains relatively stable thereafter. The RSB is the only biochar to maintain a high flowrate for an extended period of time. Its reactivity is enhanced by its high AAEM content and porous structure which enables steam to penetrate deep into its pores without much resistance. In contrast, the WPB with its low AAEM content and non-porous structure displayed the lowest reactivity following its initial devolatilisation. The low carbon content skews the product flowrates of the SSB but Fig. 3e reveals that its reactivity is high and comparable to MCB. Sewage sludge biochar on its own may not be ideal for gasification but it could be used in co-gasification mixtures to enhance low reactivity biochars. In all cases, the reactivities of the biochars decrease as conversion increases, contradicting previous studies which have shown the opposite [19] [20]. This could be as a result of the following factors; the type of biochars used, the temperature used in the formation of the biochars or it could be due to the gasification method. In the two studies mentioned, the biochars were first heated to desired temperature before steam was introduced, in this study, the biochars were introduced into a reactor at 850 °C and the sudden introduction into such an environment could have an effect on their structure and reactivity, however,

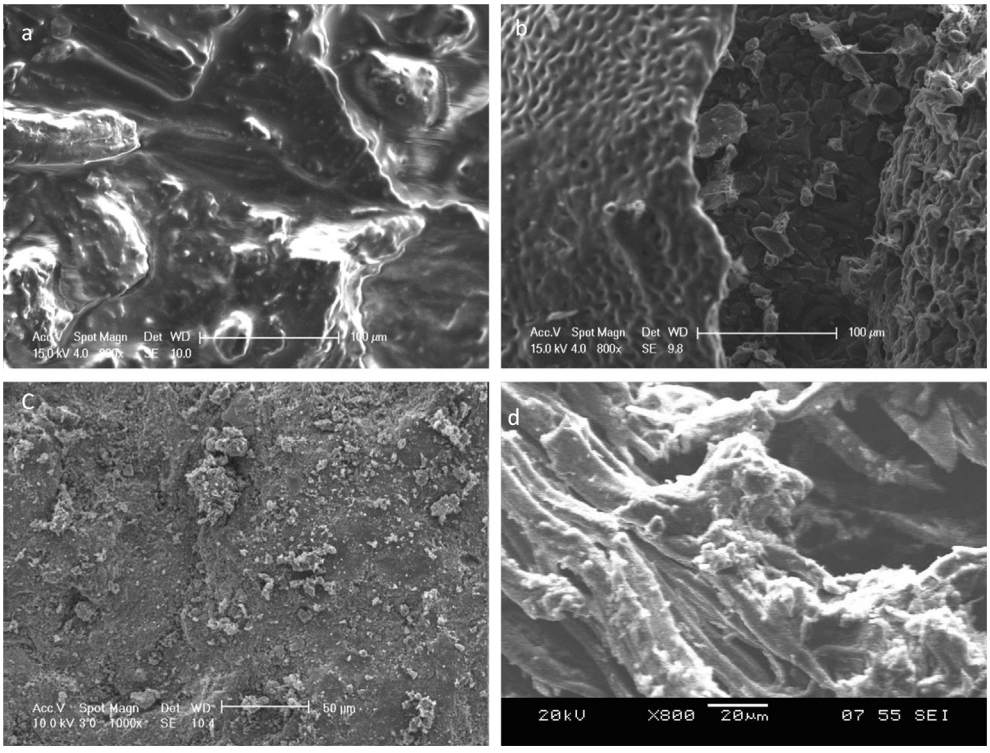


Fig. 2 – SEM analysis of the biochars. a) WPB 800X, b) RSB 800X, c) SSB 1000X, d) MCB 800X.

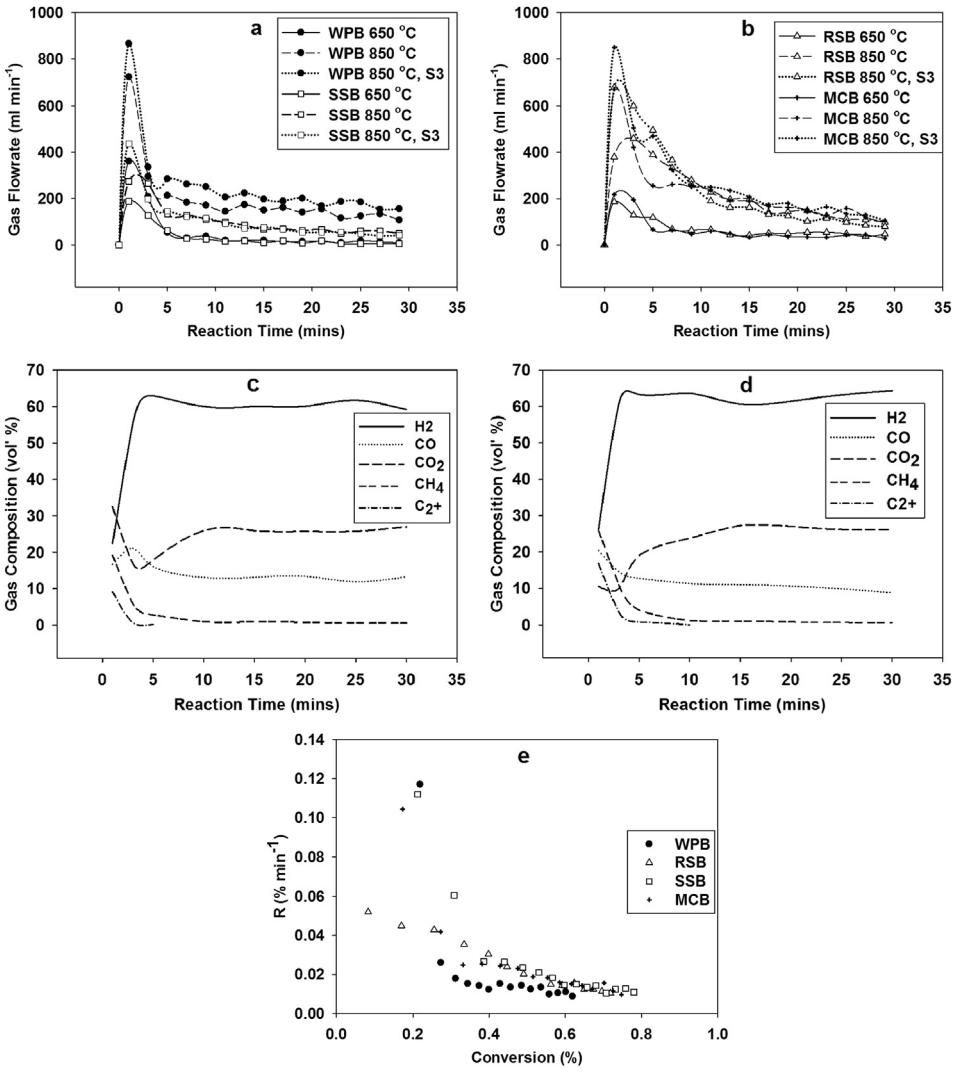


Fig. 3 – Dynamic Aspects of the gasification process; a and b) Product flow profiles of the biochars; c and d) changes in gas composition with time for SSB and WPB respectively (at 850 °C) and e) change in reactivity of the biochars with conversion (850 °C), not including carbon lost as tar. Steam flow = 172 g min^{-1} kg^{-1} biochar and S3 = 277 g min^{-1} kg^{-1} biochar.

further work is required to validate this. When conversion reaches 60% by mass, the reactivities of the biochars converge, possibly as a result of drastic changes to their structural compositions [15] indicating that mineral content and structure play a lesser role after this point. At higher steam flows, only the WPB consistently maintains an elevated product flow for the duration of the reaction (compared to lower steam flows) suggesting that it needs a higher steam-to-carbon ratio (S/C) to make up for its lack of reactivity.

3.3.1. *Changes in gas composition with time*

The dynamic behaviour of the composition during biochar gasification was previously poorly understood. Previous work has focused mainly on the final composition of the gas and not the changes that occur during the reaction. An understanding of the dynamic behaviour is essential in optimising the process for a specific need. From Fig. 3c and d, it can be seen that the dynamic behaviour of the gas composition is similar for both SSB and WPB and although not shown, it is also similar for the other biochars. As the feed is placed into the reactor, devolatilisation occurs, producing a gas which is a mixture of hydrocarbons, CO, CO_2 and H_2. The H_2 volume fraction is generally low in the initial stages as the CO, CO_2 and hydrocarbons dominate. The oxygen present in the biochar is quickly used up to form CO and CO_2 with the CO_2 further reacting with the carbon to form CO. Reaction 4 is particularly prominent at this stage (especially at higher temperatures) given that it is the fastest reaction of those given in Table 2 [8]. By the third minute, hydrogen is the dominant gas and the CO falls rapidly once the oxygen in the biochar is consumed. The hydrocarbons quickly fall off as the pyrolysis gas exits the system and reaction 3 becomes the main reaction, producing CO and H_2. Once the CO is generated, it reacts with H_2O via reaction 6 to form CO_2 and H_2. The volume fraction of CO_2 continues to rise as a result of two factors; (i) the carbon in the char decreases with time yet the steam flow remains constant so in reality, the steam-to-carbon (S/C) ratio increases as the reaction proceeds and (ii) the decrease in carbon ensures that

reaction 2 occurs less frequently even though it may be thermodynamically favourable at high temperatures. After 10 min, the system has stabilised and no significant further changes to the composition occur. The above description is similar for other temperatures but the time it takes to reach the stable state decreases with increasing temperature and at lower temperatures, the hydrocarbons are produced for a slightly longer time.

3.4. *Effects of temperature on gas composition*

The effect of temperature on the gas composition was investigated from 650 to 850 °C. The steam flow was kept constant at 172 g min^{-1} kg^{-1} biochar (S2). Data repeatability for the final gas composition was within ±4% volume fraction.

3.4.1. *Effects on hydrogen*

From Fig. 4a, it is shown that for all the biochars except WPB, hydrogen volume fraction reaches a maximum at 700 or 750 °C. This indicates the dominance of the water gas shift reaction (WGSR) which begins to reverse at temperatures above 706 °C [21]. The WPB shows an increase in hydrogen volume fraction from 30% to 53% at 650–850 °C respectively. At low temperatures, low reaction rates coupled with a large amount of hydrocarbon-containing gas produced in the initial stages, ensures that for the WPB, the initial gas has a disproportionately weighted effect on the overall composition. At higher temperatures, hydrocarbons are cracked into H_2, CO and CO_2 while simultaneously, gasification reactions, such as reaction 3, become more prominent, leading to an increase in hydrogen. An important factor that determines the overall gas composition is the time it takes for reaction 5 to become the main reaction. Fig 5a shows the change in hydrogen volume fraction with time for MCB at 650–850 °C. It is observed that eventually the hydrogen volume fraction levels off at over 60%, but, the time it takes to achieve this value varies considerably. At 650 °C, it takes around 10 min but by then, most of the gas has already been produced as seen in Fig 3b, meaning that the overall hydrogen volume fraction will be lower even though conditions favour the forward WGSR. At 850 °C, the hydrogen concentration increases sharply within the first 3 min, coinciding with the peak gas flow as seen in Figs. 5a and 3b and remains high until the end of the reaction.

3.4.2. *Effects on CO*

From Fig 4b, it can be seen that the RSB and MCB show a general increase in CO volume fraction while the WPB and SSB show an initial decrease until 750 °C and increasing thereafter. The Boudouard reaction (reaction 2) becomes prominent at temperatures around 727 °C [8] indicating that most of the CO produced below 750 °C is as a result of the initial pyrolysis and reaction 4. This explains why WPB has such a high CO volume fraction at low temperatures, since; at 650 °C, it produces 68% of its total gas volume in the first 5 min. The higher CO volume fractions for RSB and MCB at higher temperatures are a result of their high AAEM contents which catalyse the oxygen-char reactions [22].

3.4.3. *Effect on CO_2*

From Fig 4c, it can be seen that all the biochars show a general decrease with increasing temperature except the WPB which shows a significant increase until 800 °C before decreasing slightly at 850 °C. The RSB, MCB and SSB follow

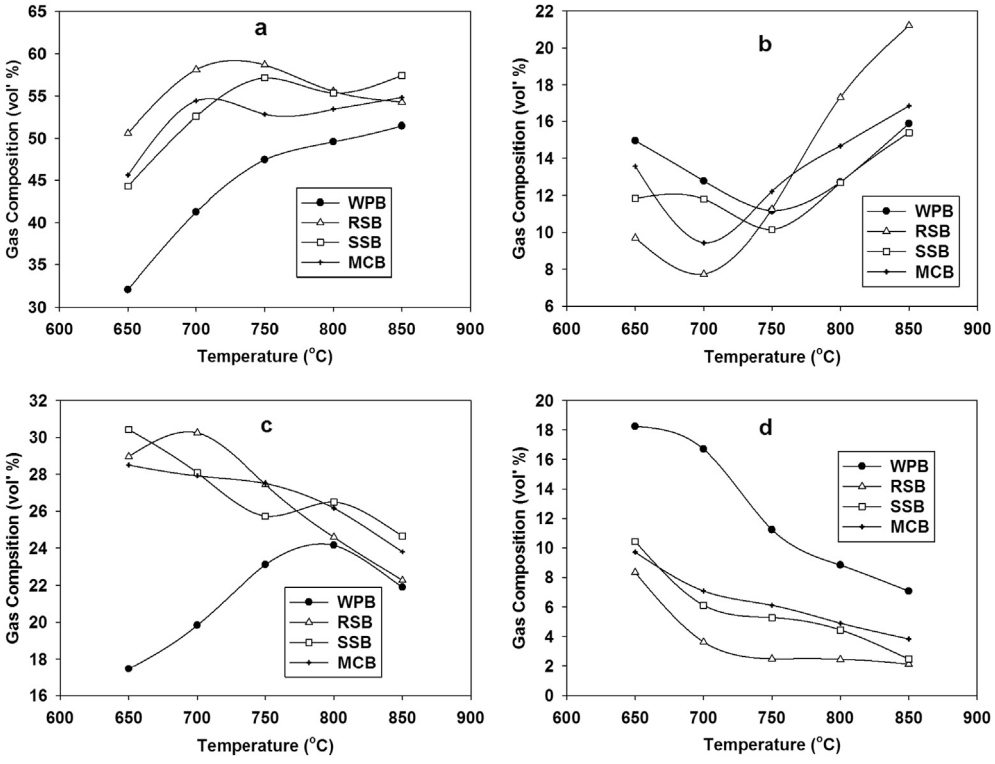


Fig. 4 – Effects of temperature on concentration for a) H_2, b) CO, c) CO_2, d) CH_4.

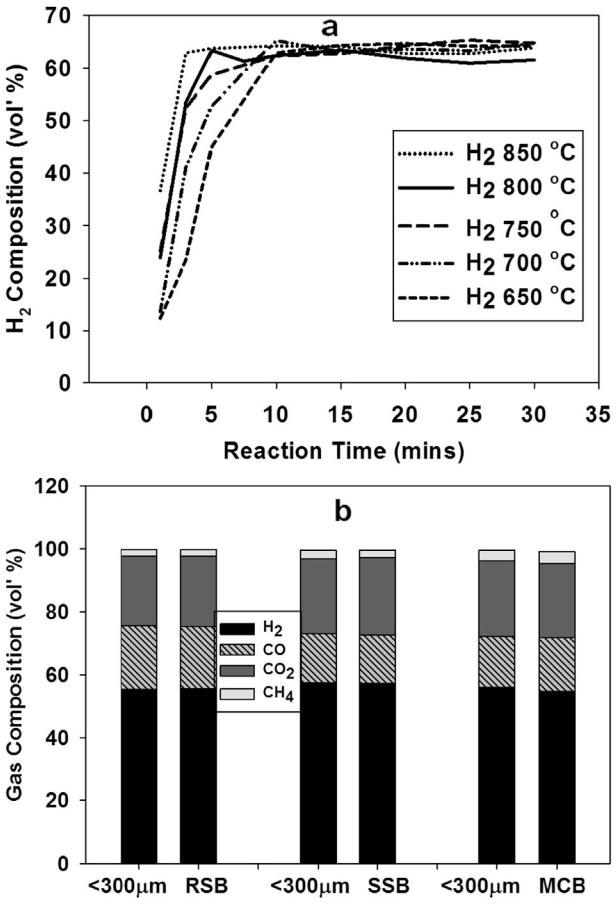


Fig. 5 – (a) Effect of temperature on hydrogen concentration with time for the MCB and (b) Effect of particle size on the gaseous composition of the biochars at 850 °C. Steam flowrate = and 172 g min^{-1} kg^{-1} biochar.

thermodynamic pathways meaning that, at higher temperatures, endothermic reactions such as reactions 2 and reverse 6 become prominent leading to a decrease in CO_2. At low temperatures, the low CO_2 volume fraction given by the WPB is explained by the high concentrations of hydrocarbons that are present. At 650 °C, hydrocarbons, excluding CH_4, accounted for 18.94% volume fraction of the total gas.

3.4.4. *Effect on CH_4*

Fig 4d shows that all the biochars display a similar behaviour as there is a general decrease with increasing temperature. Methane formation favours lower temperatures and above 624 °C, reaction 7 is unfavoured [23]. The amount of CH_4 varies with each biochar but seems to be dependent upon the volatile content. In Fig. 3c and d, high CH_4 volume fraction is observed when devolatilisation is taking place. It falls sharply when gasification reactions take over – hence, it can be concluded that the higher the volatile content, the higher the CH_4 content.

3.4.5. *Carbon conversion tar production and other effects*

Both CC and CCE are given in Table 4. The discrepancy between the two is attributed to carbon lost as tar. WPB

Table 4 – Carbon conversion, carbon conversion efficiency and associated results.

Pellet type, size fraction, temperature	Wood pellet			Rapeseed			Sewage sludge			Miscanthus			<300 μm (850 °C)		
	650 °C	750 °C	850 °C	650 °C	750 °C	850 °C	650 °C	750 °C	850 °C	650 °C	750 °C	850 °C	RSB	SSB	MCB
C_2H_6	3.26	1.08	0.38	0.60	0.03		0.82	0.41	0.03	0.56	0.23	0.35		0.05	0.04
C_2H_4	8.65	4.77	3.01	1.17	0.08	0.12	1.79	1.0	0.24	1.41	1.0	0.35	0.04	0.32	0.23
C_2+	5.35	1.19	0.30	0.60			0.42	0.28		0.62	0.12	0.03		0.03	
CC[a] (mol%)	46	61.1	87.2	29.7	54.2	90	34.4	60.3	89.8	34.8	59.6	87.9	86.2	81.8	80.7
CCE[b] (mol%)	27.3	37.2	64.3	28.3	52.2	80.9	29.3	53.8	73.1	28.9	52.1	82.5	83.3	78.9	78.6
DGY[c] (m^3 kg^{-1})	0.57	1.13	2	0.71	1.6	2.23	0.36	0.78	1.05	0.67	1.38	2.31	2.27	1.14	2.3
HHV[d] (MJ m^{-3})	27.6	16.2	13.8	13.6	10.1	10.5	13.4	11.7	11.1	11.7	12.1	10.4	10.5	10.6	10.8
H_2/CO ratio	1.98	5.36	3.47	5.1	5.5	2.8	2.86	5.57	3.72	3.22	4.23	3.26	2.75	3.7	3.68

[a] Carbon conversion, see Equation 8.
[b] Carbon conversion efficiency, see Equation 9.
[c] Dry gas yield, corrected to 298 K, 101.3 kPa see Equation 11.
[d] Higher heating value (MJ m^{-3}) see Equation 10.

generated the most tar as it consistently displayed the largest difference, and at 850 °C it amounted to 22.9%. The tar manifests itself as a black layer, deposited on the cooler parts of the sample holder and reactor as well as a thin layer of oil floating on the condensate. Dry gas yield increases with increasing temperature in all cases as a result of an increase in the rate of reaction 3. At 850 °C, the highest gas yield was obtained from the MCB at 2.31 $m^3\ kg^{-1}$, followed by the RSB at 2.23 $m^3\ kg^{-1}$ whilst the lowest was from SSB at 1.05 $m^3\ kg^{-1}$. The hydrocarbon content decreases with increasing temperature as a result of thermal cracking. The conditions seem to favour the formation of alkenes, in particular C_2H_4 as all the biochars display a high volume fraction at lower temperatures. Hydrocarbons above C_2 are generally made up of C_3H_8 and C_3H_6 but the volume fractions of these gases are very low and normally below 1% except in the case of low temperature WPB experiments. Higher heating value decreases with increasing temperature, mainly as the result of a reduced hydrocarbon content [11].

3.5. *Effects of particle size*

The size of the biochar particles has very little effect on the composition of the gas as seen in Fig. 5b as the compositions are almost identical to the original particles. These results confirm previous reports that particle size has little effect on gaseous composition at high temperatures [10], and further extends it as it has now been shown that even inconsistent particle sizes produce similar results (refer to Table 4). There is little effect on the carbon conversion efficiency as only a slight increase was observed in RSB and SSB whilst a decrease was observed in the MCB.

3.6. *Effect of steam flow on gas composition*

For the steam experiments, the temperature was kept constant and the steam flow was varied between 54 (S1) and 277 (S3) g $min^{-1}\ kg^{-1}$ biochar. Data repeatability for the final gas composition was within ±4% volume fraction.

From Fig. 6a–d, it can be seen that the composition of gases for each type of biomass follow similar trends in most cases for increases in steam flow. The hydrogen volume fraction increases in all cases (refer to Fig 6a) except for the SSB where there is little change from 56.6% at S1 to 56.8% at S3. This could be due to its low carbon content resulting in a high S/C ratio even at low steam flows. The increase in H_2 for the other biochars can be attributed mainly to reactions 5 and 6 – this is indicated by the decrease in CO and CH_4 and the increase in CO_2 (refer to Fig. 6b–d). It can be seen in Table 5 that there was very little change in the hydrocarbon content with increased steam flow. It could be due to the hydrocarbons being produced in the very early stages of the reaction when the product flowrate is very high and hence the residence time of the gases in the reactor may be too short for thermal and hydrocracking to occur. The main aim of the steam experiments was to investigate the conditions that would produce the highest hydrogen volume fraction as well as giving the highest CCE at a constant temperature of 850 °C. The carbon conversion efficiency increased with increasing steam flow – this was expected as steam is one of the main reactants. The mechanism for the steam–biochar reaction is that steam reacts with the outer surface first before entering into the pores and reacting with the inside where the surface area is much higher [8]. At low steam flows, it is likely the steam is used up by the carbon active sites on the surface, leaving the inner parts

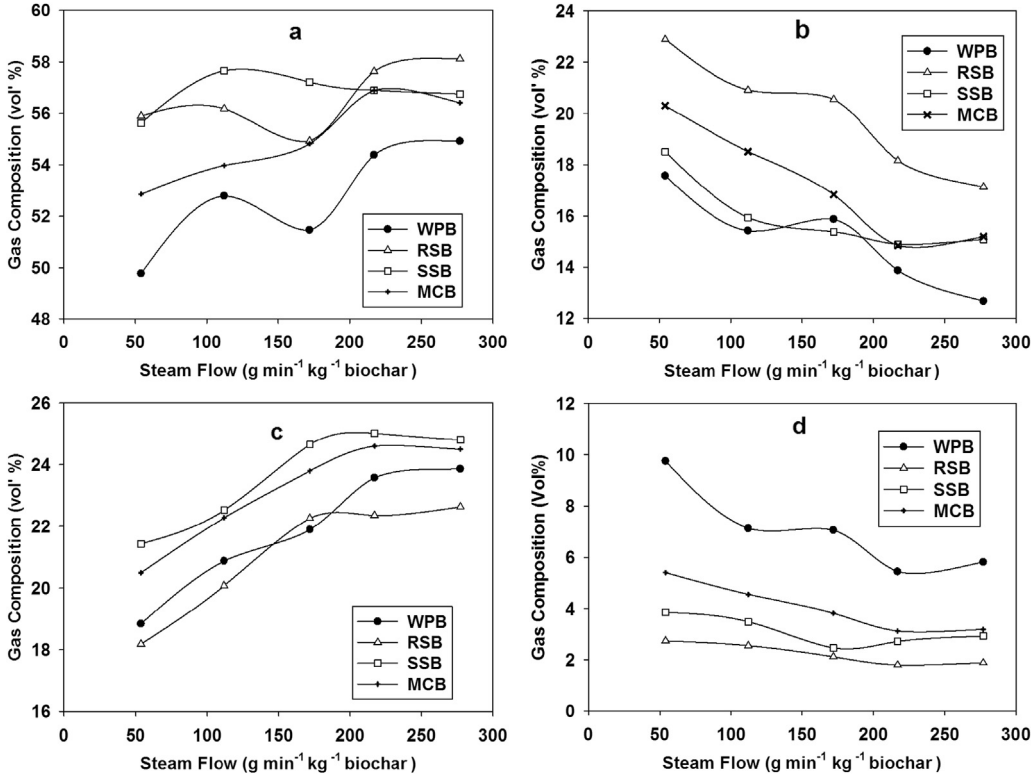


Fig. 6 – The Effects of Steam flow on the Gaseous Composition of the biochars. a) H_2, b) CO, c) CO_2 and d) CH_4.

Table 5 – Carbon conversion, carbon conversion efficiency and associated results.

	Wood pellet		Rapeseed		Sewage sludge		Miscanthus	
	S1	S3	S1	S3	S1	S3	S1	S3
C_2H_6	0.43	0.27	0.02		0.05	0.18	0.11	0.05
C_2H_4	3.29	2.2	0.25	0.19	0.48	0.22	0.75	0.52
C_2+	0.33	0.24	0.01		0.31	0.02	0.05	0.18
CC[a] (%)	78	94.9	75.2	87.2	72.8	88.4	64	84.3
CCE[b] (%)	54.3	75.6	55.8	83	55.6	75.6	60.5	84.1
DGY[c] ($m^3\ kg^{-1}$)	1.66	2.58	1.55	2.43	0.78	1.08	1.7	2.46
HHV[d] ($MJ\ m^{-3}$)	15.12	12.74	11.3	10.5	12.1	10.9	12.08	10.6
H_2/CO ratio	2.83	4.3	2.44	3.39	3.06	3.75	2.60	3.71

Where S1 and S3 are steam flows of 54 and 277 g min^{-1} kg^{-1} biochar.
[a] Carbon conversion, see Equation 8.
[b] Carbon conversion efficiency, see Equation 9.
[c] Dry gas yield, corrected to 298 K, 101.3 kPa, see Equation 11.
[d] Higher heating value, see Equation 10.

unconverted. Low steam flows also hinders reaction 6 hence the lower hydrogen and CO_2 concentrations. The highest carbon conversion, 94.9%, was achieved by the WPB at S3. This flow rate did not achieve the highest carbon conversion for all the biochars yet the difference between the carbon conversion and carbon conversion efficiency was reduced in all cases. With respect to carbon conversion efficiency, MCB was the best as it achieved a CCE of 84.1% at 277 g min^{-1} kg^{-1} biochar (S3) and its carbon conversion efficiencies were generally the closest to its carbon conversion for all the steam flows. This indicates either that it had the least amount of tar or that its tar was the easiest to crack. A possible benefit is that for biochars such as the MCB, a high flow rate of steam may negate the need for a catalyst thereby reducing costs. The highest gas yield, 2.58 $m^3\ kg^{-1}$, was obtained from WPB at S3, although there was still 19.3% difference between the carbon conversion and the carbon conversion efficiency, meaning one of two things; (i) a higher S/C ratio is needed or (ii) a catalyst is needed, such as dolomite which has been shown to be effective in cracking tars as well as improving gas yields [24].

The end-use of a particular syngas is determined by its H_2/CO ratio. For example; a high H_2/CO ratio is needed in upgrading the syngas for fuel cell use or a low H_2/CO ratio of 2:1 can be used in Fischer–Tropsch reactions [7]. Gas produced at 750 °C would be most suitable for upgrading as it consistently gave the highest H_2/CO ratio. However, the quantity of gas produced at this temperature is low. The H_2/CO ratio increased at higher steam flows with WPB producing the highest ratio at 4.3:1 at S3. The lowest ratios were given by the RSB at 2.44, 2.67 and 3.39 at S1, S2 and S3 respectively. The results indicate that the different biochars may be best suited for different end applications. For example, WPB produces a syngas with the highest heating value and H_2/CO ratio; it is therefore best suited for upgrading purposes as well as CHP applications. RSB at low to intermediate steam flows produces a syngas that could be suitable for Fischer–Tropsch reactions.

4. Conclusions

Four biochars formed via intermediate pyrolysis were gasified to produce a hydrogen-rich syngas. The dynamic aspects of the gasification process were studied as well as the effects of temperature and steam flow. It was found that the gas composition changes with time and the reactivity decreases as the reaction proceeds. All the biochars produced a high quality syngas but the quantities varied with sewage sludge biochar producing the least volume and the wood pellet biochar producing the most at 277 g min^{-1} kg^{-1} biochar steam flow. Hydrogen volume fraction reaches a maximum at 700–750 °C, whilst changing the particle size has very little effect on the syngas composition at 850 °C. Biochars in pellet form were easiest to handle but the most suitable biochars for hydrogen production were the rapeseed and miscanthus biochars.

Acknowledgements

This study was funded by the Engineering and Physical Sciences Research Council (EPSRC) grant number EP/G037116/1.

Nomenclature

WPB	Wood pellet biochar
RSB	Rapeseed biochar
MCB	Miscanthus biochar
SSB	Sewage Sludge Biochar
X	Conversion (%)
CC	Carbon conversion (%)
CCE	Carbon conversion efficiency (%)
DGY	Dry gas yield (kg m^{-3})
HHV	Higher heating value (MJ m^{-3})
S1, S2, S3	Steam flows of 54, 172 and 277 g min^{-1} kg^{-1} biochar respectively
S/C ratio	Steam-to carbon-ratio
R	Reactivity (% min^{-1})

REFERENCES

[1] Macleay I, Harris K, Annut A. Digest of united kingdom energy statistics. In: DECC. London: National Statistics; 2012.

[2] Bridgwater AV. Review of fast pyrolysis of biomass and product upgrading. Biomass Bioenergy 2012;38(0):68–94.
[3] Basu P. Chapter 5-Pyrolysis. In: Basu P, editor. Biomass gasification, pyrolysis and torrefaction. 2nd ed. Boston: Academic Press; 2013. p. 147–76.
[4] Wild PD. Biomass pyrolysis for chemicals [Doctor of Philosophy]. Groningen: University of Groningen; 2011.
[5] Mahmood ASN, Brammer JG, Hornung A, Steele A, Poulston S. The intermediate pyrolysis and catalytic steam reforming of brewers spent grain. J Anal Appl Pyrolysis 2013;103(0):328–42.
[6] Ouadi M, Brammer JG, Yang Y, Hornung A, Kay M. The intermediate pyrolysis of de-inking sludge to produce a sustainable liquid fuel. J Anal Appl Pyrolysis 2013;102(0):24–32.
[7] Chaudhari ST, Bej SK, Bakhshi NN, Dalai AK. Steam gasification of biomass-derived char for the production of carbon monoxide-rich synthesis gas. Energy Fuels 2001;15(3):736–42.
[8] Basu P. Chapter 7-gasification theory. In: Basu P, editor. Biomass gasification, pyrolysis and torrefaction. 2nd ed. Boston: Academic Press; 2013. p. 199–248.
[9] Yan F, Luo S-Y, Hu Z-Q, Xiao B, Cheng G. Hydrogen-rich gas production by steam gasification of char from biomass fast pyrolysis in a fixed-bed reactor: influence of temperature and steam on hydrogen yield and syngas composition. Bioresour Technol 2010;101(14):5633–7.
[10] Yan F, Zhang L, Hu Z, Cheng G, Jiang C, Zhang Y, et al. Hydrogen-rich gas production by steam gasification of char derived from cyanobacterial blooms (CDCB) in a fixed-bed reactor: influence of particle size and residence time on gas yield and syngas composition. Int J Hydrogen Energy 2010;35(19):10212–7.
[11] Chaudhari ST, Dalai AK, Bakhshi NN. Production of hydrogen and/or syngas (H2 + CO) via steam gasification of biomass-derived chars. Energy Fuels 2003;17(4):1062–7.
[12] Zhang S, Ma Z, Xie S, Yan Y, Ren Z. Hydrogen production from bio-char via steam gasification in a fluidized-bed reactor. Chem Eng Technol 2013;36(9):1599–602.
[13] Chen G, Yu Q, Sjöström K. Reactivity of char from pyrolysis of birch wood. J Anal Appl Pyrolysis 1997;40–41(0):491–9.
[14] ASTM. Standard test method for chemical analysis of wood charcoal D1762-84, vol. 2007. ASTM, West Conshohocken, PA (USA): American Society for Testing and Materials; 2013.
[15] Keown DM, Hayashi J-I, Li C-Z. Drastic changes in biomass char structure and reactivity upon contact with steam. Fuel 2008;87(7):1127–32.
[16] Kajita M, Kimura T, Norinaga K, Li C-Z, Hayashi J-I. Catalytic and noncatalytic mechanisms in steam gasification of char from the pyrolysis of biomass. Energy Fuels 2010;24(1):108–16.
[17] Saw W, McKinnon H, Gilmour I, Pang S. Production of hydrogen-rich syngas from steam gasification of blend of biosolids and wood using a dual fluidised bed gasifier. Fuel 2012;93(1):473–8.
[18] Brewer CE, Schmidt-Rohr K, Satiro JA, Brown RC. Characterization of biochar from fast pyrolysis and gasification systems. Environ Prog Sustain Energy 2009;28(3):386–96.
[19] Liliedahl T, Sjöström K. Modelling of char-gas reaction kinetics. Fuel 1997;76(1):29–37.
[20] Wu H, Yip K, Tian F, Xie Z, Li C-Z. Evolution of char structure during the steam gasification of biochars produced from the pyrolysis of various mallee biomass components. Ind Eng Chem Res 2009;48(23):10431–8.
[21] O'Hayre R, Cha S-W, Colella W, Prinz FB. Fuel cell fundamentals. New Jersey: Wiley; 2009.
[22] Zolin A, Jensen A, Jensen PA, Frandsen F, Dam-Johansen K. The influence of inorganic materials on the thermal deactivation of fuel chars. Energy Fuels 2001;15(5):1110–22.
[23] Kongvui Y, TiaN F, Jun-Ichiro H, Wu H. Effect of alkali and alkaline earth metallic species on biochar reactivity and syngas compositions during steam gasification. Energy Fuels 2009;24:173–81.
[24] Sutton D, Kelleher B, Ross J. Review of literature on catalysts for biomass gasification. Fuel Process Technol 2001;73:155–73.



https://dspace.org/

Steam gasification of rapeseed, wood, sewage sludge and miscanthus biochars for the production of a hydrogen-rich syngas

Sattar, Anwar; Leeke, Gary A.; Hornung, Andreas; Wood, Joseph

2014-08-20
Elsevier
http://dx.doi.org/10.1016/j.biombioe.2014.07.025.
Anwar Sattar, Gary A. Leeke, Andreas Hornung, Joseph Wood, Steam gasification of rapeseed, wood, sewage sludge and miscanthus biochars for the production of a hydrogen-rich syngas, Biomass and Bioenergy, Volume 69, October 2014, Pages 276-286

Downloaded from a DSpace repository. https://dspace.org/